doi:10.14311/ppt.2023.2.107
Plasma Physics and Technology **10**(2):107–110, 2023

INFLUENCE OF OXYGEN-CONTAINING FILLING GAS MIXTURES ON THE INTERRUPTION CAPABILITY OF MV LOAD BREAK SWITCHES

M. Castiñeira Suárez[a,*], T. Ballweber[a], A. Moser[a], M. Schaak[b], K. Ermeler[c]

[a] *Institute of High Voltage Equipment and Grids, Digitalization and Energy Economics, RWTH Aachen University, Schinkelstr. 6, 52056 Aachen, Germany*

[b] *Siemens AG, Energy Management Division, Carl-Benz-Str. 22, 60386 Frankfurt am Main, Germany*

[c] *Siemens AG, Energy Management Division, Nonnendammallee 104, 13629 Berlin, Germany*

[*] m.suarez@iaew.rwth-aachen.de

Abstract. Nowadays SF_6 is commonly used as filling gas for medium voltage load break switches due to its outstanding insulating and arc-quenching properties. However, due to its high global warming potential the interrupting performance of alternative eco-friendly gases are investigated for such devices. This contribution investigates the thermal interruption capability of a medium voltage load break switch using two different oxygen-containing gas mixtures: dry air and a mixture of nitrogen, oxygen and carbon dioxide. The findings indicate an improved performance in comparison to pure nitrogen when considering an admixture of oxygen. In gas mixtures containing 80% nitrogen, the addition of oxygen results in an enhanced thermal interruption capability compared to an equivalent proportion of carbon dioxide.

Keywords: load break switch, medium voltage, SF_6 alternatives, thermal interruption capability.

1. Introduction

Medium voltage (MV) load break switches (LBS) are frequently used in ring main units (RMU) to interrupt load currents up to 1.25 kA and serve as disconnector switches. To optimize space utilization, LBSs are typically installed in enclosed compartments as gas-insulated switchgear (GIS). The prevalent choice for filling gas has been SF_6, owing to its outstanding insulating and arc-quenching capabilities. However, SF_6 is characterized by an exceptionally high global warming potential (GWP) of 23,500 times that of carbon dioxide (CO_2) [1]. Atmospheric gases such as nitrogen (N_2), mixtures of N_2 and oxygen (O_2) or CO_2 have a lower dielectric strength compared to that of SF_6 [2]. Consequently, the design of switchgear utilizing these gases must be appropriately adapted to compensate for the lower insulation performance. This can be accomplished through increased enclosure pressure and/or insulation distance [3].

Existing research studies have shown good interruption capability when utilizing mixtures of N_2 and CO_2 in combination with arc blowing through a polymer nozzle [4–6]. However, soot formation could be observed after conducting the experimental investigations. This issue has also been encountered when mixing perfluoronitriles or perfluoroketones with CO_2. In such cases, the admixture of a small percentage of O_2 allows minimizing the generation of solid byproducts such as carbon deposits [7, 8]. The same approach is worth investigating for N_2–CO_2 mixtures, but it is essential to ensure that the resulting gas provides a sufficient interruption capability.

The present study aims to investigate the thermal interruption capability of a MV-LBS based on the design proposed by [5], with the incorporation of an O_2 admixture. Specifically, two gas mixtures are investigated, N_2–O_2 and N_2–O_2–CO_2 with ratios of 80/20 and 80/10/10 respectively. In assessing the thermal interruption capability of different gases, the arcing time constant τ_{arc} serves as an indicator [9]. This parameter represents the time constant that characterizes the change in arc voltage resulting from a step current [10]. As shown in Table 1, O_2 exhibits a smaller τ_{arc} compared to that of N_2 and CO_2. This suggests that the addition of O_2 in the gas mixture may result in improved performance compared to some of the previously studied mixtures.

Gas	Time constant [µs]
N_2	210
CO_2	15
O_2	1.5
Air	20

Table 1. Arc time constants for 1 A arc [10, 11]

2. Method

The interruption process in a LBS can be divided into two stages, namely the thermal and dielectric phases [10, 12, 13]. The present work focuses on the thermal phase.

2.1. Thermal interruption capability

When the LBS is opened, an electric arc is ignited across its contacts. In case of a successful interruption the arc is extinguished at the current zero (CZ) crossing, and the recovery voltage (RV) builds up across the open contacts. The thermal phase takes place immediately or a few microseconds after CZ [10]. The residual conductivity in the switching gap results in a small post-arc current (PAC) as the RV rises. For a successful interruption, cooling power must exceed the power input of the PAC. In gas switches, this is accomplished by blowing cool gases into the switching chamber. If the cooling power is insufficient, the conductivity and PAC increase lead to a thermal reignition [13]. In this contribution, the accuracy of the current measurement is not sufficient for examining the PAC.

The investigation method, presented in detail in [4], is summarized in the following. The current steepness shortly before CZ ($\mathrm{d}i/\mathrm{d}t_{\mathrm{CZ}}$) is used to quantify the thermal interruption capability of the LBS.

Figure 1 shows the test circuit used for the investigation of the thermal interruption capability, consisting of two resonant circuits. Initially, the high-current circuit is used to generate a 50 Hz sinusoidal current representing the load current I_{hc}. The injection circuit provides a higher frequency current I_{inj}. Shortly before CZ, the thyristor of the injection circuit is triggered and I_{inj} is superimposed to I_{hc}. This approach allows the investigation of varying $\mathrm{d}i/\mathrm{d}t_{\mathrm{CZ}}$ independently of the load current, by adjusting the charging voltage of C_V. If the arc is extinguished at the first CZ of I_{inj}, the RV builds up as I_{inj} charges the capacitor C_p through the resistor R_p. Contrarily, if the arc is re-ignited a second oscillation of the I_{inj} flows through the open contacts of the LBS. To ensure the rate of rise of recovery voltage (RRRV) characteristic of a 24 kV grid at 50 Hz when setting the current steepness of a typical load current of 630 A, a resistor $R_p = 220\,\Omega$ is chosen. Figure 2 shows a comparison of voltage and current for a current interruption in the first and second CZ respectively.

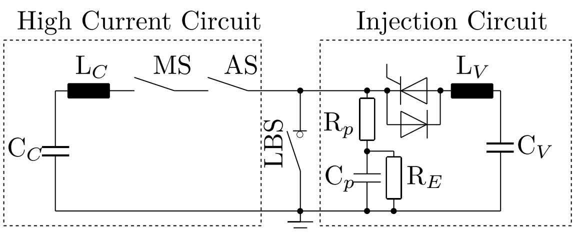

Figure 1. Synthetic test circuit for investigation of thermal interruption capability [5].

At the beginning of a test series a low $\mathrm{d}i/\mathrm{d}t$ is set by using a small charging voltage for C_V and five tests are conducted. If all five tests result in a successful interruption, the charging voltage is increased by $\Delta U = 500\,\mathrm{V}$ and another series of five tests is performed. This procedure is repeated until a charging

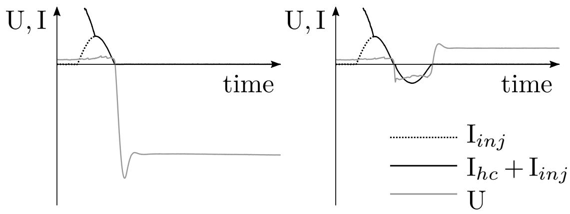

Figure 2. Current and voltage in the vicinity of CZ during thermal interruption test.

voltage level is reached where at least one test results in a failed interruption. The critical current steepness at CZ crossing ($\mathrm{d}i/\mathrm{d}t_{\mathrm{crit}}$) is determined as the mean value between the lowest $\mathrm{d}i/\mathrm{d}t_{\mathrm{CZ}}$ corresponding to a failed interruption and that of the next successful interruption below. This value defines the limit for safe operation of the LBS.

2.2. Model switch

A simplified cross-sectional view of the model switch is depicted in Figure 3. The switch consists of a pin-tulip contact system made of a tungsten-copper (WCu) alloy with 80/20 weight ratio. The pin contact has a diameter of $d_{\mathrm{c}} = 10\,\mathrm{mm}$. Surrounding the contact system is a polymeric nozzle made of PTFE, with a throat diameter of $d_{\mathrm{n}} = 11\,\mathrm{mm}$ and a throat length of $l_{\mathrm{n}} = 24\,\mathrm{mm}$. These dimensions have been derived as part of a parameter study presented in [5].

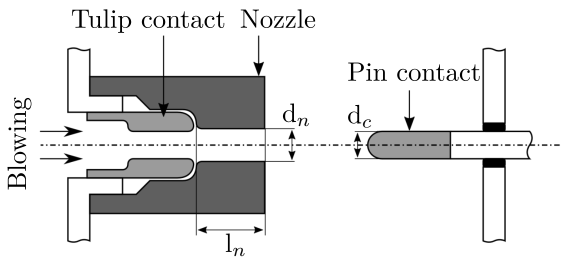

Figure 3. Section of the model load break switch [4, 6].

The contact system and the nozzle are enclosed in a pressurized main vessel with a volume of $V = 150\,\mathrm{l}$ at 1.8 bar of absolute pressure. An external tank is used to provide the blowing pressure for cooling the arc. The main vessel and the external tank are connected via a magnetic valve that is opened shortly before the contacts start separating to initiate the gas flow. The pressure inside the blowing tank is adjusted accordingly to investigate different blowing pressure levels. The pressure is measured upstream the contact system, behind the magnetic valve. A pneumatic drive with a total stroke of 107 mm is used to achieve the opening motion of the contact system. The mean opening speed is set to $v_{\mathrm{mean}} = 5\,\mathrm{m/s}$. A laser sensor measures the position of the pin contact throughout the opening motion.

Figure 4 displays typical voltage and current values measured during an exemplary interruption test using the provided setup, as well as the travel signal representing the separation of contacts.

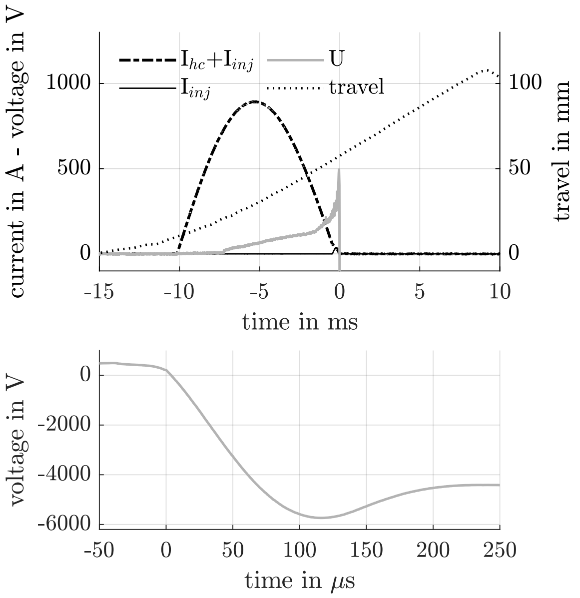

Figure 4. Typical current, voltage and travel signals for an exemplary interruption test (top) and recovery voltage (bottom).

3. Results and discussion

Figure 5 presents the critical current steepness of the two gas mixtures investigated in this study, namely N_2–O_2 (80/20) and N_2–O_2–CO_2 (80/10/10), as a function of blowing pressure. The investigation has been performed with the same test setup and conditions as [6]. In order to compare the results to the gas mixtures previously studied, the figure includes results from the mentioned paper. Specifically pure N_2 and N_2 with admixtures of 20%, 40% and 60% CO_2. Lines connecting the data points are drawn for visualization and do not correspond to actual data.

The two mixtures investigated in this study show a linear increase in $\mathrm{d}i/\mathrm{d}t_{\mathrm{crit}}$ with blowing pressure. This tendency goes in line with the results obtained for N_2–CO_2. Similarly, mixtures containing 60% of N_2 or more resulted in a linear behavior. The admixture of higher percentages of CO_2 contributed to an exponential increase. In the two mixtures containing O_2, the required $\mathrm{d}i/\mathrm{d}t_{\mathrm{CZ}}$ of 0.28 A/μs ($\mathrm{d}i/\mathrm{d}t_{\mathrm{target}}$) for a LBS with a rated load current of 630 A and a voltage level of 24 kV at 50 Hz is achieved with a blowing pressure of 660 mbar. Both mixtures exhibit improved thermal interruption capability compared to pure N_2, but are outperformed by mixtures containing 40% CO_2 or more.

Moreover, the N_2–O_2 (80/20) mixture results in a better interruption capability than the gas mixture containing 10% CO_2. The difference in performance could be attributed to the τ_{arc} of O_2 and CO_2. A small τ_{arc} indicates a faster change in temperature of the arc [10]. The higher concentration of O_2, with a τ_{arc} ten times shorter compared to CO_2, may result in

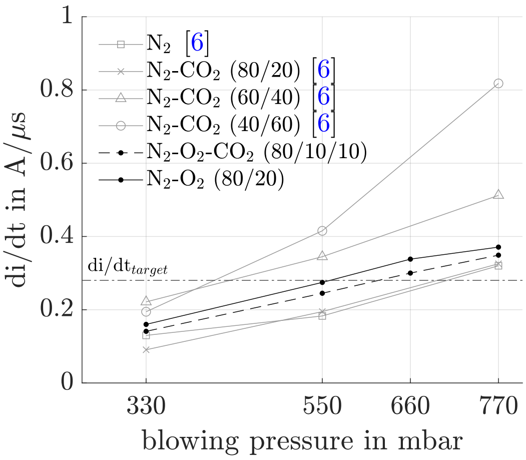

Figure 5. Critical current steepness for various gas mixtures and blowing pressures.

a faster reduction of the arc conductance. This could also explain why the addition of a 20% CO_2 has a minor effect on the interruption capability compared to pure N_2, whereas the admixture of the same percentage in O_2 results in a significant improvement in performance.

Nevertheless, τ_{arc} is not sufficient as a quantification parameter for the interrupting capability of a particular gas. As indicated in Table 1, both CO_2 and air exhibit comparable τ_{arc}. However, existing research shows that pure CO_2 leads to a significantly higher $\mathrm{d}i/\mathrm{d}t_{\mathrm{crit}}$ compared to the results obtained in this contribution for air [13]. Furthermore, it must be considered that τ_{arc} is dependent on the current magnitude [10]. The investigations presented in this work are performed using a 50 Hz current with $I_{\mathrm{rms}} = 630$ A, whereas the values presented in Table 1 were obtained for 1 A arcs.

As shown in Figure 4 (top), a steep voltage increase takes place shortly before CZ as part of the extinction peak. The successful current interruption relies on the formation of a high extinction peak and thus on the cooling before CZ [13]. Therefore a comparison of the extinction peak voltage for both gases investigated is of interest.

Figure 6 shows the extinction peak in dependence of current steepness. The results are grouped into sets of four data points within a 5 mA/μs range. The circles represent the mean extinction peak voltage for each set and the horizontal markers the maximum and minimum values. The extinction peaks are shown for interruption tests performed with a blowing pressure of $p_{\mathrm{B}} = 330$ mbar (top) and $p_{\mathrm{B}} = 660$ mbar (bottom).

For 330 mbar, higher extinction peak voltages can be observed for N_2–O_2 in the current steepness range where the $\mathrm{d}i/\mathrm{d}t_{\mathrm{crit}}$ of the worse performing gas is found ($\mathrm{d}i/\mathrm{d}t \approx 0.14$ A/μs). However, since the scattering of the voltages measured for both gases overlap, no clear relation between extinction peak and $\mathrm{d}i/\mathrm{d}t_{\mathrm{crit}}$ can be derived for this pressure level. This could explain the small difference in $\mathrm{d}i/\mathrm{d}t_{\mathrm{crit}}$ of both gases for

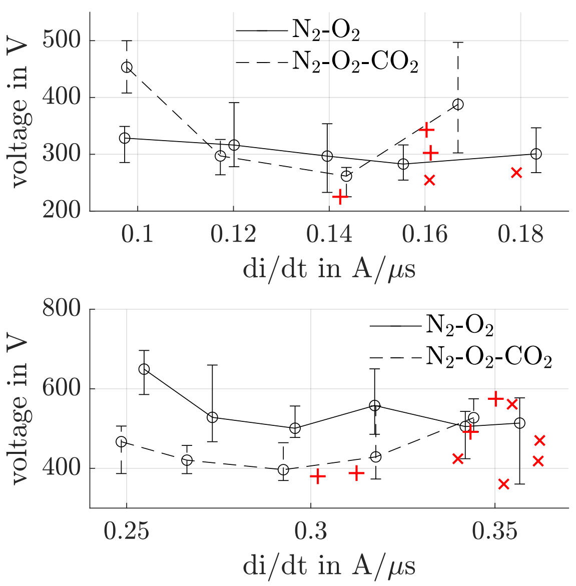

Figure 6. Extinction peak voltage using a blowing pressure of 330 mbar (top) and 660 mbar (bottom). Red crosses and plus signs correspond to individual tests resulting in failed interruption for N_2–O_2 and N_2–O_2–CO_2 respectively.

this p_B value.

For $p_B = 660$ mbar there is a significant difference in the extinction peak voltage measured for both gases. The mean of the voltages measured for N_2–O_2 is approximately 100 to 130 V higher until $\mathrm{d}i/\mathrm{d}t \approx 0.32$ A/µs. The lower extinction peak measured for N_2–O_2–CO_2 could be related to a higher arc conductivity shortly before CZ and thus a worse cooling performance, which could explain the lower $\mathrm{d}i/\mathrm{d}t_{\mathrm{crit}}$.

The incorporation of O_2 into the gas mixture provides beneficial effects in the thermal interruption capability. Nevertheless, it is important to consider that O_2 exhibits strong oxidizing properties [8]. The potential drawbacks associated with its oxidizing nature should be carefully evaluated before implementing such mixtures in practical applications.

4. Conclusion

This study presents an investigation on the thermal interruption capability of a model LBS using two gas mixtures containing O_2: N_2–O_2 (80/20) and N_2–O_2–CO_2 (80/10/10). The influence of blowing pressure can be examined through implementation of an external vessel. The results indicate that the addition of O_2 improves the interruption capability compared to pure N_2 or N_2 with comparable CO_2 percentages. The gas mixtures containing 40% CO_2 or more result in superior performance. Substituting CO_2 with an equivalent ratio of O_2 may potentially enhance the interruption capability further. However, it is crucial to consider the long-term effects of O_2 due to its strong oxidizing properties, which could pose challenges in practical applications. Further investigation of the dielectric recovery phase is necessary to evaluate the performance of these gases during the complete current interruption process.

References

[1] G. Myhre et al. Anthropogenic and natural radiative forcing. In *Climate Change 2013: The Physical Science Basis. Contribution of Working Group I to the Fifth AR of the IPCC*. Cambridge University Press, 2013. ISBN 978-92-9169-138-8.

[2] D.-Y. Lim and S. Bae. Study on oxygen/nitrogen gas mixtures for the surface insulation performance in gas insulated switchgear. *IEEE Transactions on Dielectrics and Electrical Insulation*, 22(3):1567–1576, 2015. doi:10.1109/TDEI.2015.7116352.

[3] L. Niemeyer. A systematic search for insulation gases and their environmental evaluation. In *Gaseous Dielectrics VIII*, pages 459–464. Springer-Verlag, 1998. ISBN 978-0-306-46056-2.

[4] M. Bendig et al. Investigations on the effect of the nozzle material on the interruption capability of a medium voltage load break switch. *Plasma Physics and Technology*, 6(1):15–18, 2019. doi:10.14311/ppt.2019.1.15.

[5] M. Bendig and M. Schaak. Design rules for environmentally friendly medium voltage load break switches. *IEEE Transactions on Power Delivery*, 36(5):1–9, 2020. doi:10.1109/TPWRD.2020.3024983.

[6] T. Krampert et al. Influence of the filling gas mixture on the interruption capability of medium voltage load break switches. *Plasma Physics and Technology*, 8(2):19–22, 2021. doi:10.14311/ppt.2021.2.19.

[7] M. Seeger, R. Smeets, J. Yan, et al. Recent development of alternative gases to SF_6 for switching applications. *Electra (CIGRE)*, 2017.

[8] F. Ye, X. Zhang, C. Xie, et al. Effect of oxygen and temperature on thermal decomposition characteristics of $C_4F_7N/CO_2/O_2$ gas mixture for MV equipment. *IEEE Access*, 8:221004–221012, 2020. doi:10.1109/ACCESS.2020.3043334.

[9] T. Uchii, T. Shinkai, and K. Suzuki. Thermal interruption capability of carbon dioxide in a puffer-type circuit breaker utilizing polymer ablation. In *IEEE/PES Transmission and Distribution Conference and Exhibition*, volume 3, pages 1750–1754, 2002. doi:10.1109/TDC.2002.1177719.

[10] K. Niayesh. *Power Switching Components Theory, Applications and Future Trends*. Power Systems. Springer International Publishing, 2017. ISBN 978-3-319-51459-8.

[11] H. Knobloch. *The Comparison of Arc-Extinguishing Capability of Sulfur Hexafluoride (SF6) with Alternative Gases in High-Voltage Circuit-Breakers*, pages 565–571. Springer US, Boston, MA, 1998. ISBN 978-1-4615-4899-7.

[12] M. Bendig. *Ausschaltvermögen von Mittelspannungs-Lasttrennschaltern bei Verwendung atmosphärischer Lösch-und Isoliergase*. PhD thesis, RWTH Aachen University, 2020.

[13] T. Krampert. *Ausschaltverfahren von Mittelspannungslasttrennschaltern auf Basis von Stickstoff-Kohlenstoffdioxid-Mischungen*. PhD thesis, RWTH Aachen University, 2022.